Morinda officinalis oligosaccharides ameliorate corticosterone-induced depression-like behaviour in mice by modulating the BDNF signalling pathway and gut microbiota

MENGJIE HE[1*], ZIXUAN LIU[1*], YUXIN CHEN[1], XIAORU WU[2], XUELING DAI[1], QIAN LIU[1], SHUO WANG[3], ZEPING ZUO[2**] and YAXUAN SUN[1**]

[1]Beijing Key Laboratory of Bioactive Substances and Functional Food, College of Biochemical Engineering, Beijing Union University, Beijing 100191, P.R. China; [2]Beijing Tongrentang Company Limited, Beijing 100062, P.R. China; [3]Tianjin Key Laboratory of Food Science and Health, School of Medicine, Nankai University, Tianjin 300350, P.R. China

Received January 28, 2026; Accepted April 24, 2026

DOI: 10.3892/mmr.2026.13948

Abstract. The aim of the present study was to elucidate the regulatory effect of *Morinda officinalis* oligosaccharides (MOOs) on the brain-derived neurotrophic factor (BDNF)/tropomyosin receptor kinase B (TrkB)/cAMP response element-binding protein (CREB) signalling pathway and the gut microbiota in a corticosterone (CORT)-induced chronic stress model. Mice received subcutaneous injections of CORT for 35 days. During this period, different concentrations of MOOs were concurrently administered by gavage. The synergistic regulatory effect of MOOs on the hippocampal BDNF/TrkB/CREB signalling pathway and gut microbiota remodelling was assessed using western blotting, ELISA, 16S ribosomal RNA sequencing, H&E/Nissl staining and reverse transcription-quantitative PCR in the CORT-induced chronic stress mouse model. In this model, MOOs alleviated depression-like behaviour, promoted the expression of BDNF and neuronal nuclear antigen in the hippocampus, normalised monoamine neurotransmitter levels in the brain, activated the BDNF/TrkB/CREB signalling pathway, increased BDNF expression in the hippocampus and remodelled the intestinal microbiota, thereby exerting antidepressant effects. These results suggested that MOOs exerted antidepressant-like effects in CORT-exposed mice by attenuating hippocampal neuronal damage, activating the BDNF/TrkB/CREB signalling pathway and ameliorating gut microbiota dysbiosis. These findings provide novel evidence for the clinical application of MOOs in depression.

Correspondence to: Ms. Zeping Zuo, Beijing Tongrentang Company Limited, 20 South Third Ring Middle Road, Fengtai, Beijing 100062, P.R. China
E-mail: zepingzuo@126.com

Professor Yaxuan Sun, Beijing Key Laboratory of Bioactive Substances and Functional Food, College of Biochemical Engineering, Beijing Union University, 18 Fatou Xili 3rd District, Chaoyang, Beijing 100191, P.R. China
E-mail: sunxx@buu.edu.cn

[*,**]Contributed equally

Key words: Morinda officinalis oligosaccharides, corticosterone, depression, neuronal injury, brain-derived neurotrophic factor, gut microbiota

Introduction

Depression is a neuropsychiatric disorder associated with persistent stress and neuronal dysfunction, typically resulting in neurological dysfunction in specific brain regions following stressful stimuli (1). Depression affects millions of individuals worldwide and puts patients at increased risk of suicide, leading to serious health and socioeconomic consequences (2). The pathogenesis of depression is complex and may be associated with low psychological and cognitive activity, and hippocampal neuronal damage due to reduced neurotransmitter levels and loss of neurotrophic factors, leading to dysregulated neuroplasticity (3) and neuroinflammation (4), as well as changes in the gut microbiota (5,6). At present, treatment for depression relies primarily on pharmacotherapy, with tricyclic antidepressants and selective serotonin (5-HT) reuptake inhibitors being commonly used classes of medications (7). However, current medications still have several limitations, including their single-target nature, a high risk of toxicity and drug resistance, and the fact that they do not exert the desired therapeutic effect in certain individuals (8). Therefore, exploring multi-pathway, relatively safe and effective antidepressant drugs is of great significance to the current research on depression. Herbal medicines have demonstrated unique advantages in this regard and have gradually become a common area of research (9).

Morinda officinalis oligosaccharides (MOOs) are bioactive compounds extracted from the root of the Chinese herb *Morinda officinalis* How (10). MOO is used as a tonic to enhance kidney function and improve sexual performance (11). In addition, MOOs exert neuroprotective effects *in vitro* and *in vivo* (12) and have also shown potent antidepressant activity in animal models of depression (13). Due to their own bioactivity, MOOs are also recognised as a functional ingredient that

promotes intestinal health (14). Notably, MOO capsules were approved as an oral prescription drug by the National Medical Products Administration of China in 2012 for the clinical treatment of mild to moderate depressive episodes, MOO clinical antidepressant efficacy has been confirmed (15). However, to the best of our knowledge, the regulatory effects of MOOs on the brain-derived neurotrophic factor (BDNF)/tropomyosin receptor kinase B (TrkB)/cAMP response element-binding protein (CREB) signalling pathway in the hippocampus and gut microbiota have not been clearly elucidated. Furthermore, in the corticosterone (CORT)-induced chronic stress depression model, the characteristics of MOO-mediated regulation of gut microbiota composition and MOO protective effect on hippocampal neurons have not been systematically verified experimentally, which provides a core entry point for the present study.

Chronic stress (for example, due to CORT administration) has been used as an animal model of depression in antidepressant studies several times (16,17). In the present study, the effects of CORT on hippocampal damage and the effects of MOO treatment were assessed by examining hippocampal neuronal morphology. In addition, the composition of the gut microbiota of mice was analysed further to elucidate its relationship with depression via the microbiota-gut-brain axis.

Materials and methods

Experimental animals. The animal experiments were approved by the Experimental Animal Ethics Committee of the Center for Health Food Functional Testing, College of Applied Arts and Sciences (Beijing Union University, Beijing, China; approval no. JCZX11-2404-1). A total of 72 healthy male 8-week-old ICR mice weighing 28-30 g were purchased from Beijing Beiyou Biological Co., Ltd. [SYXK (Beijing) 2023-0013]. All mice were housed in a specific pathogen-free-grade animal room at the Health Food Functional Testing Center, College of Applied Arts and Sciences, Beijing Union University [license no. SYXK (Beijing) 2017-0038; Beijing, China], with a 12-h light-dark cycle at a constant temperature of 22±2˚C and a relative humidity level of 45%. All mice were provided *ad libitum* access to standard laboratory chow and sterile drinking water. In this experiment, the general physiological status, fur condition, mental activity, food and water intake, and dynamic body weight changes of mice were monitored at fixed daily frequencies. Strict criteria for humane animal euthanasia endpoints were established: i) Body weight loss >20% for 3 consecutive days; ii) severe lethargy with inability to eat or drink independently; iii) occurrence of convulsions, severe physical injury or secondary infection; and iv) the animal entering an irreversible moribund state. No accidental animal deaths or unplanned premature euthanasia occurred throughout the study. The mice were anaesthetised via intraperitoneal injection of 1% sodium pentobarbital at a dose of 50 mg/kg calculated based on the body weight of the mouse. After the animal was deeply anesthetized and unconscious, euthanasia was performed by cervical dislocation. The death of animals was confirmed by cardiac arrest, cessation of spontaneous breathing and irreversible loss of the pupillary light reflex. All experimental procedures strictly complied with the 3R Principles and the Animal Research: Reporting of *In Vivo* Experiments Guidelines to minimize animal stress and suffering (18). The housing environment was maintained under standardized constant temperature and humidity conditions, and mice were housed in separate cages to prevent fighting and injury. Environmental enrichment toys were provided to enrich daily behavioural activities, fully safeguarding the welfare of laboratory animals.

Establishment of the CORT mouse model of chronic depression. CORT (MilliporeSigma) was dissolved in 0.9% saline containing 0.1% DMSO and 0.1% Tween 80, followed by sonication at 25˚C and 40 kHz for 15 min to prepare a uniform suspension. During the experimental period, each mouse not in the control group was injected subcutaneously with 40 mg/kg/day CORT solution for 35 days (19). Mice were given subcutaneous injection of CORT at a dose volume of 0.1 ml/10 g body weight. Control mice were injected with an equal volume of 0.9% saline at the same time point.

Grouping and drug administration. After 1 week of acclimation, mice were randomly divided into six groups (n=12 per group): i) Control group, given 0.9% saline by gavage; ii) CORT model group, injected subcutaneously with 40 mg/kg CORT and given 0.9% saline by gavage; iii) MOO-L group, injected subcutaneously with 40 mg/kg CORT and administered 39 mg/kg MOOs by gavage; iv) MOO-M group, injected subcutaneously with 40 mg/kg CORT and administered 78 mg/kg MOOs by gavage; v) MOO-H group, injected subcutaneously with 40 mg/kg CORT and administered 156 mg/kg MOOs by gavage; and vi) fluoxetine group, injected subcutaneously with 40 mg/kg CORT and administered 20 mg/kg fluoxetine by gavage. In the present study, fluoxetine was used as a positive control to verify the validity and reliability of the experimental model and detection system, thereby providing a reference for evaluating the antidepressant effects of MOOs. The concentration of MOOs was set based on the recommended human dose, and the concentration of fluoxetine was performed as previously described (20).

MOO capsules (batch no. 2021B03527; 0.3 g MOO capsule containing 150 mg MOOs; Beijing Tongrentang Company Limited) and fluoxetine hydrochloride (cat. no. F131623; Shanghai Aladdin Biochemical Technology Co., Ltd.) were administered in a volume of 0.1 ml/10 g once per day. The drug was administered by gavage 30 min before CORT injection for 35 days. Behavioural tests were performed on day 36, and the experimental flow chart is shown in Fig. 1A. The samples administered to each group of mice were prepared in 0.9% saline.

Behavioural tests

Sucrose preference test (SPT). The SPT is used to measure reward preference and detect depressive states such as pleasure deprivation (21). The two-bottle choice method was used to assess sucrose preference in mice. On the first day, two bottles containing 1% sucrose solution were placed in each cage for 24 h. Subsequently, the mice were subjected to a 16-h water fast. Next, the mice were provided with food and two bottles of liquid (1% sucrose solution and purified water), which were weighed, randomly placed and exchanged after 12 h to control for location effects on the choice behaviour of the mice. After 24 h, the consumption in each bottle was recorded,

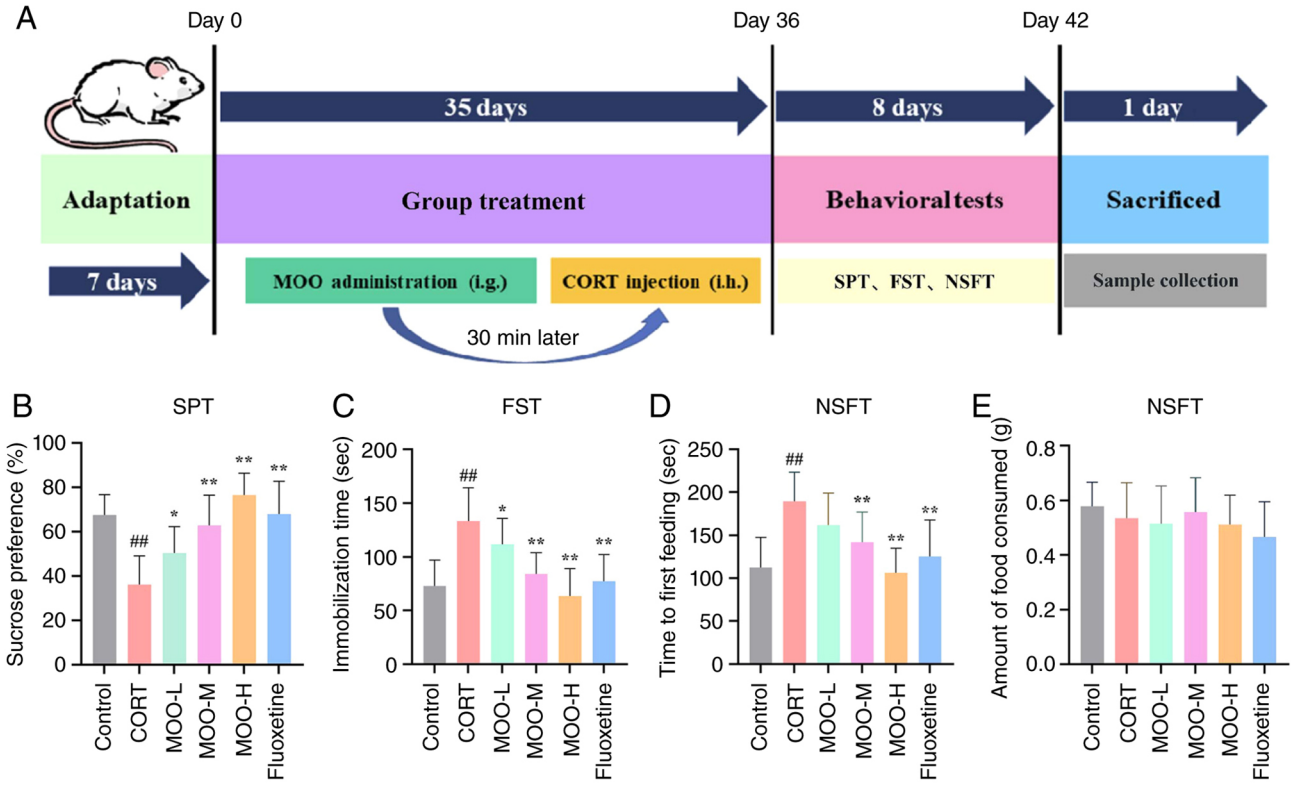

Figure 1. MOOs alleviate CORT-induced depression-like behaviour in mice. (A) Schematic diagram of the experimental flow. (B) Effect on sugar-water preference rate. (C) Effect on immobilization time in the FST. (D) Effect on time to the first meal in the NSFT. (E) Effect on food consumption in the NSFT. $^{\#\#}$P<0.01 compared with the control group. *P<0.05 and **P<0.01 compared with the CORT group. CORT, corticosterone; FST, forced swimming test; i.g., intragastric; i.h., hypodermic injection; MOO, *Morinda officinalis* oligosaccharide; MOO-H, high-dose MOO; MOO-L, low-dose MOO; MOO-M, medium-dose MOO; NSFT, novelty-suppressed feeding test; SPT, sucrose preference test.

and the sucrose preference value was calculated (22) using the following formula: Sucrose preference (%)=sucrose intake (g)/[sucrose intake (g) + water intake (g)] x100%.

Forced swimming test (FST). The FST was used to measure depressive states (behavioural despair) in animals. Mice were placed in cylindrical containers (40 cm high and 15 cm in diameter) filled with just enough water to allow them to breathe but not stand upright. On day 1, all mice were trained to swim for 15 min. On day 2, after the mice were placed in the same environment for 1 min to acclimate, the immobility time was recorded within 5 min. Immobility time was defined as the time the mice floated on the water surface, balancing only by sliding their forelimbs. The protocol was performed as described previously (23).

Novelty-suppressed feeding test (NSFT). Mice were fasted and dehydrated for 24 h, then placed in a new cage (30x30x25 cm) in the corner. Individual pelletized food was placed on a white sheet of paper in the centre of the box, and the time of the first feeding was recorded (24). Prior to the test, the food was weighed and placed in the home cages of the mice. Immediately after the test, the animals were returned to their own cages and allowed to eat for 15 min. After 15 min, the food was weighed again, and the amount of food consumed was calculated.

H&E staining. Mouse brain tissue was fixed in 4% paraformaldehyde at room temperature for 24 h, dehydrated with an ascending gradient of ethanol solutions, cleared with xylene and embedded in liquid paraffin for 90 min. Coronal sectioning was performed with a sectioning machine (Leica RM 2016; Leica Microsystems GmbH) with a section thickness of ~4 μm (25). All sections were subjected to routine H&E staining at room temperature for 5-10 min. Sections were treated with xylene and sealed with neutral adhesive. Subsequently, the pathological features of the brain tissues from mice were observed under a light microscope with panoramic section-scanning software (Pannoramic DESK/MIDI/250/1000; 3DHISTECH, Ltd.).

Nissl staining. Fixed coronal sections (4 μm) were prepared from mouse brain tissues prefixed in 4% paraformaldehyde at room temperature for 24 h, mounted on slides and baked in an oven at 65˚C for 1 h. The sections were stained with 0.5% toluidine blue O at room temperature for 10 min. The nidus was observed under a light microscope with SlideViewer (Version 2.9.0; 3DHISTECH) (26). Neurons were studied in three randomly selected fields of view and neurons with prominent nucleoli, observable rounded nuclei and intact cytoplasm with Nissl staining were counted as positive cells. Neurons with condensed cytoplasm and shrunken cytosol were considered damaged. The number of Nissl bodies in the hippocampal cornu ammonis 1 (CA1), CA3 and dentate gyrus (DG) regions was quantified using ImageJ (Version 1.54f; National Institutes of Health, USA).

Immunohistochemistry Immunohistochemistry was performed as described previously with minor modifications (26). Mouse

Table I. Primer sequences.

Gene	Forward primer (5'-3')	Reverse primer (5'-3')
GAPDH	GCAAATTCAACGGCACAGTCAAG	TCGCTCCTGGAAGATGGTGATG
BDNF	CGACGACATCACTGGCTGACAC	GAGGCTCCAAAGGCACTTGACTG
TrkB	GGTCTATGCCGTGGTGGTGATTG	CCAGCCGCTTCCTCCTTTCATG
CREB	CTGAAGAAGCAGCACGGAAGAGAG	TTCAAGCACTGCCACTCTGTTCTC

BDNF, brain-derived neurotrophic factor; CREB, cAMP response element-binding protein; TrkB, tropomyosin receptor kinase B.

brain tissue was fixed in 4% paraformaldehyde at room temperature for 24 h, dehydrated with an ascending gradient of alcohol solutions, embedded in paraffin and cut into 4 μm thick sections as described previously (27). Routine dewaxing to water was performed. Sections were heated in citrate buffer (pH 6.0) at 95-98˚C for 20 min. Sections were washed with PBS three times for 3 min each, incubated with 3% H_2O_2 for 10 min to block endogenous peroxidase activity and washed with PBS three times for 3 min each. After removing residual PBS, sections were blocked with 10% unimmunized normal sheep serum (Solarbio, Beijing, China) at 37˚C for 30 min to eliminate non-specific binding. Sections were then washed with PBS three times for 3 min each. The neuronal nuclear antigen (NeuN; 1:500; cat. no. 26975-1-AP; Proteintech Group, Inc.) and BDNF (1:500; cat. no. ab108319; Abcam) primary antibodies were added overnight at 4˚C. Goat anti-rabbit HRP-labelled secondary antibody (1:500; cat. no. SA00001-2; Proteintech Group, Inc.) was added, and the tissues were incubated at 37˚C for 60 min. Signals were developed using DAB) chromogen. Tissues were counterstained with haematoxylin at room temperature for 5 min. Sections were dehydrated through a series of descending gradient alcohol solutions, cleared using xylene and sealed with neutral resin. The pathological changes and protein expression in the hippocampal CA1, CA3 and DG regions were observed under a light microscope and analysed using the CaseViewer 2.3.0 image analysis system (3DHISTECH, Ltd.). Three consecutive different fields of view were randomly selected in each section, and the expression levels of NeuN and BDNF were quantitatively analysed using ImageJ software (Version 1.54f; National Institutes of Health, USA).

ELISA of biochemical markers in the hippocampus. A total of 100 μg protein lysate was extracted from the hippocampus using RIPA lysis buffer (cat. no. WB-0072; Beijing Dingguo Changsheng Biotechnology Co., Ltd.) and PMSF protease inhibitor cocktail (cat. no. WB-0181; Beijing Dingguo Changsheng Biotechnology Co., Ltd.). The resulting lysate was centrifuged at 5,000 x g for 5 min at 4˚C and the supernatant was collected (28). 5-HT (cat. no. CSB-E08365m), dopamine (DA; cat. no. CSB-E08661m) and norepinephrine (NE; cat. no. CSB-E07870m, all from Cusabio Technology, LLC) levels were measured in the hippocampal lysate by ELISA according to the manufacturer's instructions. The absorbance was measured at 450 nm.

Reverse transcription-quantitative PCR (RT-qPCR). RT-qPCR was used to detect the mRNA expression levels of BDNF, TrkB and CREB in the hippocampus. Total RNA was extracted from the hippocampus of mice using RNA extraction kit (cat. no. NEP017; Beijing Dingguo Changsheng Biotechnology Co., Ltd.) and RNA purity and content were assessed. RT was performed using an mRNA RT kit (TransGen Biotech Co., Ltd.) (29) at 42˚C for 15 min. The entire RT-qPCR temperature protocol was set as follows: Pre-denaturation at 95˚C for 30 sec, followed by 40 cycles of denaturation at 95˚C for 15 sec and annealing/extension at 60˚C for 30 sec. SYBR Green I fluorophore (TransGen Biotech Co., Ltd.) was used for fluorescence signal detection. Amplification was performed using a real-time fluorescent qPCR system (Anhui Wanyi Science and Technology Co., Ltd.). GAPDH was selected as the reference gene. The relative mRNA expression levels were calculated via the $2^{-\Delta\Delta Cq}$ method (30). The primer sequences are shown in Table I.

Western blotting. Western blotting was performed as described previously with minor modifications (31). Hippocampal tissue was collected and lysed with RIPA lysis buffer (cat. no. WB-0072; Beijing Dingguo Changsheng Biotechnology Co., Ltd.). Tissue homogenate was centrifuged at 5,000 x g for 15 min at 4˚C and the supernatant was collected for subsequent protein quantification using a BCA assay. After protein quantification, equal amounts of protein (40 μg of protein per lane) were separated via 10% SDS-PAGE). The separated proteins were transferred to PVDF membranes, which were blocked with 5% BSA (cat. no. FA016-100G; Genview) at room temperature for 2 h to block non-specific binding sites. The membranes were then incubated overnight at 4˚C with one of the following primary antibodies: BDNF (1:10,000; cat. no. ab108319), TrkB (1:5,000; cat. no. ab187041; Abcam), phosphorylated (p-)TrkB Tyr705 (1:1,000; cat. no. ab229908; all Abcam), CREB (1:1,000; cat. no. 9197), p-CREB Ser133 (cat. no. 9198) or β-tubulin (all 1:1,000; cat. no. 2128; all Cell Signaling Technology, Inc.). Membranes were washed three times with 0.1% TBST) and incubated with HRP-conjugated anti-rabbit IgG (H+L) secondary antibody (1:1,000; cat. no. A0208; Beyotime Biotechnology) for 2 h at room temperature. After three additional washes with TBST, protein bands were visualised using ECL (cat. no. WBKLS0100, Millipore). The grayscale values of protein bands were quantitatively analyzed using ImageJ software (Version 1.54f; National Institutes of Health).

Microbiota analysis based on 16S ribosomal RNA (rRNA) sequencing. At the end of the behavioural tests, faecal samples

from mice were collected, frozen in liquid nitrogen and stored at -80˚C until further processing. Total microbial genomic DNA was extracted from the faecal samples using a Faecal Genomic DNA Extraction Kit (cat. no. DP328; Tiangen Biotech Co., Ltd., Beijing, China) according to the manufacturer's protocol. The quality and integrity of extracted genomic DNA were assessed by 1% agarose gel electrophoresis (performed at 120 V for 20 min in 1X TAE buffer, followed by visualization with a gel imaging system) , while DNA concentration and purity were determined using a NanoDrop spectrophotometer. The highly variable V3-V4 region of bacterial 16S rRNA genes was amplified using specific forward and reverse primers: 341F (5'-CCTACGGGGNGGCWGCAG-3') and 806R (5'-GGACTACHVGGGGTATCTAAT-3'), generating a 470-bp amplicon. PCR amplification was performed using Taq DNA Polymerase (cat. no. ET101; TransGen Biotech Co., Ltd., Beijing, China). The thermocycling conditions were set as follows: initial pre-denaturation at 95˚C for 3 min; 35 cycles of 95˚C for 30 sec, 55˚C for 30 sec, and 72˚C for 45 sec and a final extension at 72˚C for 10 min. All samples were amplified in triplicate. PCR products were separated via 2% agarose gel electrophoresis and visualized using a gel imaging system, followed by gel extraction and purification. The purified amplicons were quantified using a NanoDrop spectrophotometer. The sequencing library was constructed using the TruSeq DNA PCR-Free Library Preparation Kit (cat. no. FC-121-3001; Illumina, Inc., USA). The final library concentration was measured by qPCR), and the library was loaded at a concentration of 10 nM for sequencing. Paired-end sequencing with a read length of 300 bp was performed on the Illumina MiSeq platform (Illumina, Inc., USA) using the MiSeq Reagent kit v3 (cat. no. MS-102-3003; Illumina, Inc.) for bidirectional sequencing of the V3-V4 region. Bioinformatics analysis of gut microbial community composition and diversity was performed using the NovoMagic analysis platform (Version 3.0; URL: https://magic.novogene.com). Raw sequencing data were processed through quality control, sequence splicing, and taxonomic annotation to complete the analysis of gut microbial characteristics (32). Microbial diversity and community composition analyses were performed using the integrated bioinformatics cloud platform of Novogene Co., Ltd. (Beijing, China). For α diversity analysis, the richness and diversity of microbial communities were evaluated based on the Chao1 and Shannon indices, and statistical differences among groups were analyzed to reflect the complexity of species diversity within each sample. Beta diversity was assessed to compare the similarity of microbial community structures across groups. Principal coordinate analysis (PCoA) was performed based on Bray-Curtis distance to visualize the overall differences in microbial community composition. To verify the significance of community structural differences between groups, analysis of similarities (ANOSIM) and permutational multivariate analysis of variance (ADONIS) were conducted using permutation tests. ANOSIM was used to evaluate the degree of difference between and within groups, while ADONIS was applied to quantify the interpretation degree of grouping factors for microbial community variation and assess the statistical significance of differences. PetalPlot analysis was performed using R software (Version 4.2.1; The R Foundation for Statistical Computing) to systematically display the composition, distribution and relative abundance of dominant microbial taxa at multiple taxonomic levels. Linear discriminant analysis (LDA) effect size (LEfSe) analysis was finally carried out to screen biomarker species with significant differences among groups. The linear discriminant analysis (LDA) threshold was set to identify significantly differential taxa, which could characterize the specific microbial biomarkers responding to experimental treatments.

Statistical analysis. Statistical analysis was performed using SPSS version 10.0 (SPSS, Inc.) and graphs were generated using GraphPad Prism version 9.0 (Dotmatics). Data are presented as the mean ± standard deviation of three independent biological replicates. Differences between groups were assessed using one-way ANOVA, followed by Tukey's post hoc multiple comparison test. $P<0.05$ was considered to indicate a statistically significant difference.

Results

MOOs alleviate CORT-induced depression-like behaviour in mice. Following 35 days of exposure to CORT and MOO treatments, there was a significant difference in sucrose preference between groups. Compared with the control group, mice exposed to CORT exhibited significantly lower sucrose preference in behavioural tests ($P<0.01$; Fig. 1B), suggesting that CORT induced depressive behaviours in mice. Sucrose preference was significantly higher in the MOO-L, MOO-M, MOO-H and fluoxetine groups compared with the CORT group (MOO-L, $P<0.05$; MOO-M, $P<0.01$; MOO-H, $P<0.01$; Fluoxetine, $P<0.01$). In the FST, there were significant differences in immobilisation time among the groups (Fig. 1C). The immobilisation time of mice in the CORT group was significantly higher compared with that of mice in the control group ($P<0.01$), while different doses of MOOs and Fluoxetine significantly reduced the immobilisation time of mice exposed to CORT compared with that in the CORT group (MOO-L, $P<0.05$; MOO-M, $P<0.01$; MOO-H, $P<0.01$; Fluoxetine, $P<0.01$). In the NSFT, the time to first feeding of mice in the CORT group was significantly longer than that of the control group ($P<0.01$, Fig. 1D), whereas treatment with medium and high doses of MOOs and fluoxetine significantly shortened the time to first feeding of CORT-induced mice (MOO-L, $P>0.05$; MOO-M, $P<0.01$; MOO-H, $P<0.01$; fluoxetine, $P<0.01$). There were no significant differences among the groups of mice in terms of food consumption within 15 min after returning to their own cages ($P>0.05$; Fig. 1E). Overall, these results suggested that MOOs reversed CORT-induced depression-like behaviour in mice.

MOOs ameliorate CORT-induced histopathological changes and neuronal damage in the mouse hippocampus. H&E staining was used to assess the effects of different treatments on hippocampal histopathology. The results of H&E staining showed that neuronal cells in the CA1, CA3 and DG regions of the hippocampus of the control group were uniformly distributed, tightly arranged in a well-ordered manner, exhibited a physiologically normal structure without cytosolic wrinkles or deep staining phenomena, and possessed a clearly defined structure of the nuclear membrane and nucleolus, indicative

of normal growth of neurons in the hippocampus of these mice (Fig. 2A). However, the CORT group exhibited neuronal structural ambiguities, enlarged gaps, and a loose and disorganized arrangement in the CA1, CA3 and DG regions, with notable cytosolic nuclear crumpling and cytosolic vacuolation phenomena, indicative of mild lesions and neuronal cell damage. Compared with the CORT group, the structural abnormalities were reduced following MOO treatment at different doses and fluoxetine. The morphological integrity of neurons in the CA1, CA3 and DG regions of the hippocampus increased, and disorganisation, aberrant arrangement and cytosolic vacuolization decreased in a dose-dependent manner.

Nissl staining was used to assess morphological changes in hippocampal neurons and to determine whether MOOs could ameliorate CORT-induced hippocampal neuronal injury. The results of Nissl staining showed that in the hippocampal CA1, CA3 and DG regions of control mice, neurons were arranged regularly with clear cell boundaries. Nissl bodies were intact and evenly distributed in the cytoplasm (Fig. 2B). Compared with the control, the hippocampal CA1, CA3 and DG regions of mice in the CORT group exhibited disintegration of Nissl vesicles and a significant reduction in the number of Nissl vesicles (CA1, $P<0.01$; CA3, $P<0.01$; DG, $P<0.01$; Fig. 2C-E), suggesting that CORT promoted hippocampal neuronal damage. Compared with the CORT group, different doses of MOOs and fluoxetine alleviated neuronal damage in hippocampal CA1 (all $P<0.01$), CA3 (MOO-L, $P<0.01$; MOO-M, $P<0.01$; MOO-H, $P<0.01$; Fluoxetine, $P<0.01$) and DG (MOO-L, $P<0.01$; MOO-M, $P<0.01$; MOO-H, $P<0.01$; Fluoxetine, $P<0.01$) regions, based on the significant increase in the number of Nissl vesicles. These results suggested that MOOs attenuated CORT-induced neuronal damage in the mouse hippocampus.

MOOs reverse CORT-induced downregulation of NeuN and BDNF in the mouse hippocampus. To further confirm whether MOOs improved CORT-induced neuronal damage in the hippocampus, the expression of the neuron-specific nuclear protein NeuN in the hippocampal CA1, CA3 and DG regions was assessed using immunohistochemistry. The CORT group exhibited a significant reduction in NeuN-positive expression in the pyramidal layer of hippocampal CA1, CA3 and DG regions compared with the control group (CA1, $P<0.01$; CA3, $P<0.01$; DG, $P<0.01$; Fig. 3A and C-E). Compared with the CORT group, administration of different doses of MOOs and Fluoxetine resulted in significant increases in the expression levels of NeuN in mouse hippocampal CA1 (MOO-L, $P<0.01$; MOO-M, $P<0.01$; MOO-H, $P<0.01$; Fluoxetine, $P<0.01$), CA3 (MOO-L, $P<0.01$; MOO-M, $P<0.01$; MOO-H, $P<0.01$; Fluoxetine, $P<0.01$) and DG (MOO-L, $P<0.01$; MOO-M, $P<0.01$; MOO-H, $P<0.01$; fluoxetine, $P<0.01$) regions. NeuN was expressed in neuronal cytoplasm, and the positive cells exhibited a yellowish-brown colour. These results indicated that MOOs exerted neuroprotective effects on CORT-induced damage in mice.

BDNF protein expression in the CA1, CA3 and DG regions of the hippocampus after CORT and MOO treatment was subsequently assessed by immunohistochemistry. The BDNF-positive immunoreactive products were brownish-yellow or brown in colour and were centrally located in the cytoplasm and around the nuclear membranes in the form of a ring. Compared with those in the control group, the expression levels of BDNF in hippocampal CA1, CA3 and DG regions (CA1, $P<0.01$; CA3, $P<0.01$; DG, $P<0.01$; Fig. 3B and F-H) were significantly lower in the CORT group. Compared with the CORT group, MOOs and Fluoxetine significantly increased the BDNF protein expression levels in hippocampal CA1 (MOO-L, $P<0.01$; MOO-M, $P<0.01$; MOO-H, $P<0.01$; Fluoxetine, $P<0.01$), CA3 (MOO-L, $P<0.01$; MOO-M, $P<0.01$; MOO-H, $P<0.01$; Fluoxetine, $P<0.01$) and DG (all $P<0.01$) regions. These results suggested that MOOs promoted the growth and development of hippocampal neurons in CORT-induced depressed mice, contributed to neurogenesis, and thus, exerted antidepressant effects.

MOOs regulate the activity of the BDNF/TrkB/CREB signalling pathway. To further investigate the effects of MOOs on hippocampal neurons, the mRNA and protein expression levels of genes and proteins involved in the BDNF/TrkB/CREB signalling pathway were examined. RT-qPCR results showed that the mRNA expression levels in the hippocampus of BDNF ($P<0.01$; Fig. 4A), TrkB ($P<0.01$; Fig. 4B) and CREB ($P<0.01$; Fig. 4C) were significantly downregulated in the mice in the CORT group compared with the control group. Treatment with medium and high doses of MOOs and Fluoxetine significantly upregulated BDNF (MOO-L, $P>0.05$; MOO-M, $P<0.05$; MOO-H, $P<0.01$; Fluoxetine, $P<0.05$), TrkB (MOO-L, $P>0.05$; MOO-M, $P<0.05$; MOO-H, $P<0.01$; Fluoxetine, $P<0.01$) and CREB (MOO-L, $P>0.05$; MOO-M, $P<0.05$; MOO-H, $P<0.01$; fluoxetine, $P<0.01$) mRNA expression in the hippocampus compared with that in the CORT group. These results suggested that MOOs reduced depression by regulating the mRNA expression levels of members of the BDNF/TrkB/CREB signalling pathway.

Western blotting results demonstrated that the BDNF ($P<0.01$; Fig. 4D), p-TrkB/TrkB ($P<0.01$; Fig. 4E) and p-CREB/CREB ($P<0.01$; Fig. 4F) levels in the hippocampus were significantly reduced in the CORT group compared with the control group. After MOO administration at medium, high doses and Fluoxetine, compared with the CORT group, the levels of BDNF (MOO-L, $P<0.01$; MOO-M, $P<0.01$; MOO-H, $P<0.01$; Fluoxetine, $P<0.01$), p-CREB/CREB (MOO-L, $P>0.05$; MOO-M, $P<0.01$; MOO-H, $P<0.01$; Fluoxetine, $P<0.01$) and p-TrkB/TrkB (all $P<0.01$) in the hippocampus were increased. These results suggested that MOOs may alleviate depressive symptoms by regulating signalling in the BDNF/TrkB/CREB pathway, thereby modulating neuroplasticity to exert antidepressant-like effects.

MOOs reverse CORT-induced downregulation of monoamine neurotransmitter levels in the hippocampus. In the present study, an ELISA was used to assess the effects of MOOs on monoamine neurotransmitter levels in the hippocampus. 5-HT ($P<0.05$; Fig. 5A), DA ($P<0.05$; Fig. 5B) and NE ($P<0.01$; Fig. 5C) levels in the hippocampus of CORT mice were significantly lower than those in the control group. The CORT-induced decrease in hippocampal 5-HT levels was significantly reversed by medium and high doses of MOOs and fluoxetine (MOO-L, $P>0.05$; MOO-M, $P<0.05$; MOO-H, $P<0.01$; Fluoxetine, $P<0.01$). DA and NE levels were also elevated (MOO-L, $P>0.05$; MOO-M, $P<0.05$; MOO-H, $P<0.01$; Fluoxetine, $P<0.01$).These results suggested that MOOs may ameliorate depression by modulating the monoamine neurotransmitterergic system.

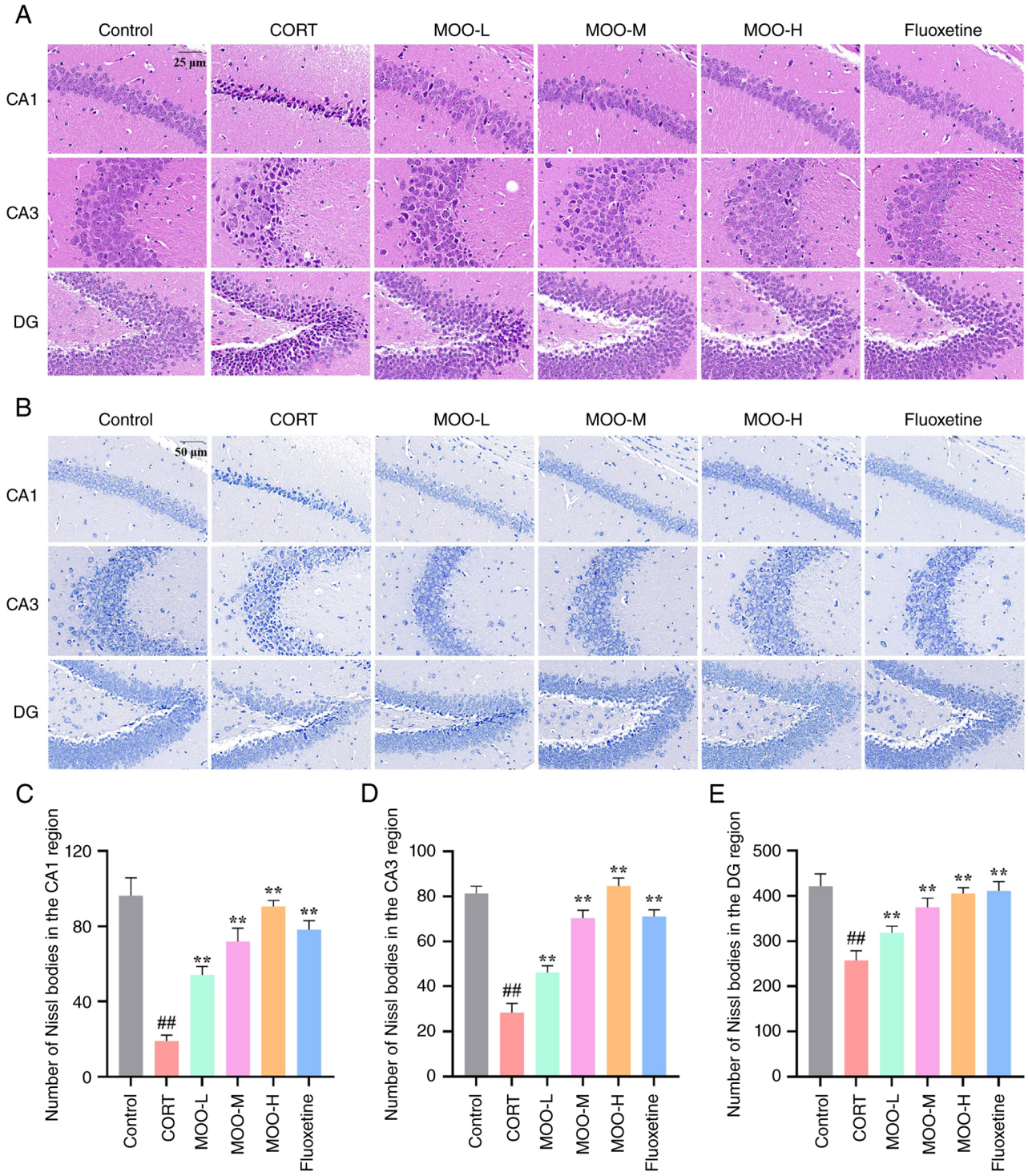

Figure 2. MOOs ameliorate CORT-induced histopathological changes and neuronal damage in the mouse hippocampus. (A) H&E staining was used to observe histopathological changes in hippocampal CA1, CA3 and DG regions. Scale bar, 20 μm. (B) Nissl staining was performed to observe neuronal changes in hippocampal CA1, CA3 and DG regions. Scale bar, 50 μm. Number of Nissl-positive cells in hippocampal (C) CA1, (D) CA3 and (E) DG regions. $^{\#\#}$P<0.01 vs. control. **P<0.01 compared with the CORT group. CA1, cornu ammonis 1; CORT, corticosterone; DG, dentate gyrus; MOO, *Morinda officinalis* oligosaccharide; MOO-H, high-dose MOO; MOO-L, low-dose MOO; MOO-M, medium-dose MOO.

Effect of MOOs on CORT-induced dysbiosis in mice

MOOs modulate gut microbiota diversity in CORT-induced mice. High-throughput sequencing of full-length 16S rRNA from mouse faeces was performed to analyse the effect of MOOs on CORT-induced dysbiosis in mice. First, comparisons of operable taxonomic units (OTUs) of gut microorganisms were performed using the obtained feature sequences, which were subjected to PetaPlot analysis. The number of feature sequences common to all groups was 201. A total of 152 feature sequences were unique to the control group, 90 feature sequences were unique to the CORT group, 87 feature sequences were unique to the MOO-L group, 228 feature sequences were unique to the MOO-M group, 148 feature sequences were unique to the MOO-H group and 195 feature sequences were unique to

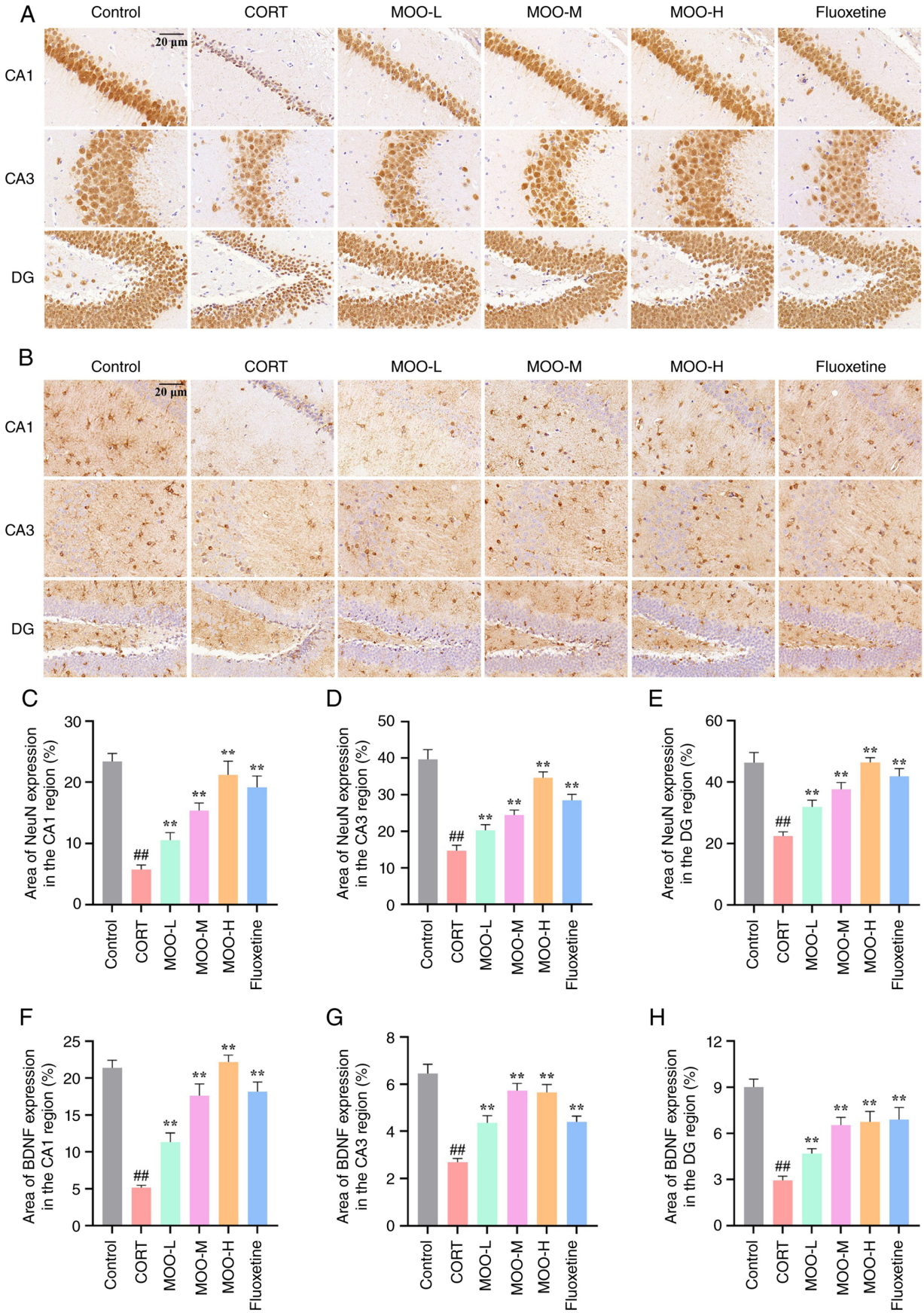

Figure 3. Effect of MOOs on CORT-induced downregulation of NeuN and BDNF expression in the mouse hippocampus. (A) Immunohistochemistry was performed to observe changes in NeuN expression in the hippocampal CA1, CA3 and DG regions. (B) Immunohistochemistry was used to observe changes in BDNF expression in the hippocampal CA1, CA3 and DG regions. Scale bar, 20 μm. Expression levels of NeuN in the hippocampal (C) CA1, (D) CA3 and (E) DG regions. Expression levels of BDNF in the hippocampal (F) CA1, (G) CA3 and (H) DG regions. $^{\#\#}$P<0.01 compared with the control group. **P<0.01 vs. CORT group. BDNF, brain-derived neurotrophic factor; CA1, cornu ammonis 1; CORT, corticosterone; DG, dentate gyrus; MOO, *Morinda officinalis* oligosaccharide; MOO-H, high-dose MOO; MOO-L, low-dose MOO; MOO-M, medium-dose MOO; NeuN, neuronal nuclear antigen.

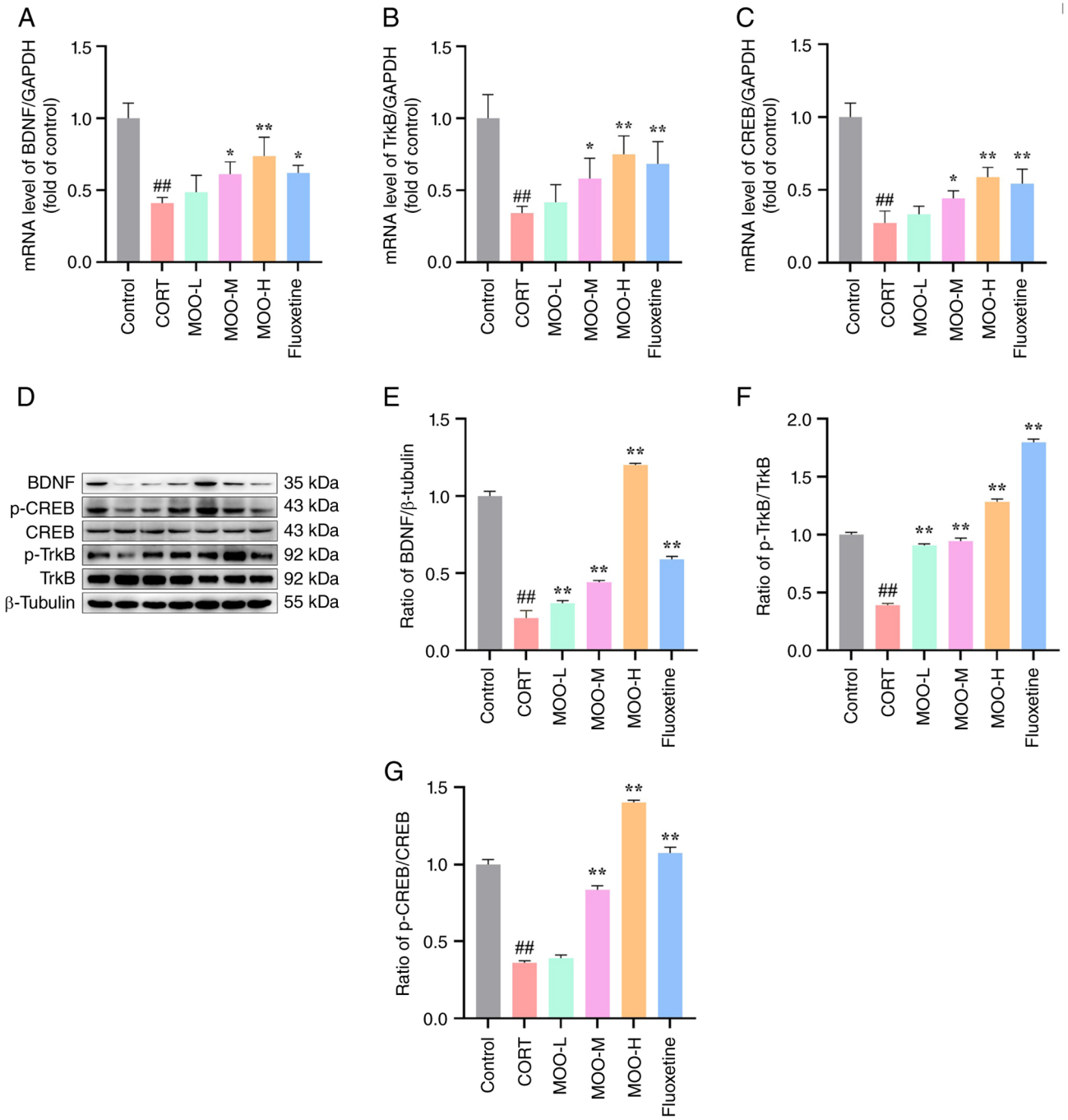

Figure 4. MOOs regulate the activity of the BDNF/TrkB/CREB signalling pathway. Reverse transcription-quantitative PCR was performed to assess the mRNA expression levels of (A) BDNF, (B) TrkB and (C) CREB in the hippocampus. (D) Western blotting was performed to assess the protein expression levels of BDNF, p-TrkB/TrkB and p-CREB/CREB in the hippocampus. Semi-quantification of (E) BDNF, (F) p-TrkB/TrkB and (G) p-CREB/CREB protein experession in the hippocampus $^{\#\#}$P<0.01 compared with the control group. *P<0.05 and **P<0.01 vs. CORT group. BDNF, brain-derived neurotrophic factor; CORT, corticosterone; CREB, cAMP response element-binding protein; MOO, *Morinda officinalis* oligosaccharide; MOO-H, high-dose MOO; MOO-L, low-dose MOO; MOO-M, medium-dose MOO; p-, phosphorylated; TrkB, tropomyosin receptor kinase B.

the fluoxetine group (Fig. 6A). Anosim and Adonis analyses showed that gut microbiota composition in the control mice was significantly different from mice in the CORT, as well as between the MOO, fluoxetine group and the CORT group (Fig. 6B).

The α-diversity analysis revealed the abundance and diversity of gut microbial communities across the six sample groups. The α-diversity analysis results showed that, compared with the control group, in the CORT group, the Chao (P<0.01; Fig. 6C) and Shannon (P<0.01; Fig. 6D) indices were significantly lower, whereas the Simpson index (P<0.01; Fig. 6E) was significantly higher, indicating relatively low microbial abundance. When compared with the CORT group, medium and high doses of MOOs and Fluoxetine resulted in a relatively high microbial abundance. The Chao (MOO-L, P>0.05; MOO-M, P<0.05; MOO-H, P<0.01; Fluoxetine, P<0.01) and Shannon (MOO-L, P>0.05; MOO-M, P<0.01; MOO-H, P<0.01; Fluoxetine, P<0.01) indices were significantly higher,

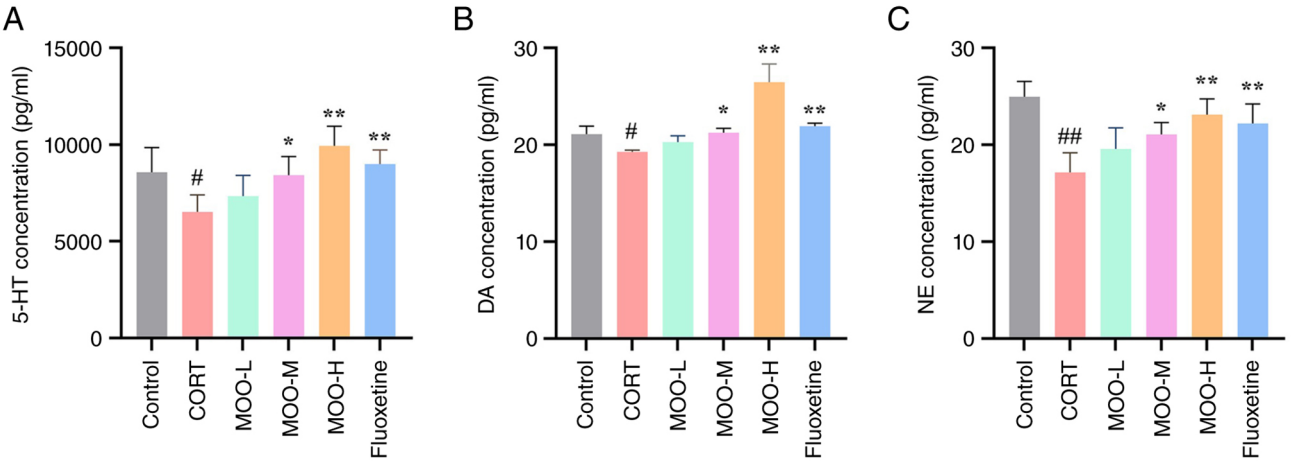

Figure 5. Effect of MOOs on CORT-induced downregulation of neurotransmitter levels in the hippocampus. Changes in the levels of (A) 5-HT, (B) DA and (C) NE in the hippocampus. All data are presented as the mean ± standard deviation (n=3). P<0.05 was considered to indicate a statistically significant difference. $^{\#}$P<0.05 and $^{\#\#}$P<0.01 compared with the control group. *P<0.05 and **P<0.01 compared with the CORT group. 5-HT, serotonin; CORT, corticosterone; DA, dopamine; MOO, *Morinda officinalis* oligosaccharide; MOO-H, high-dose MOO; MOO-L, low-dose MOO; MOO-M, medium-dose MOO; NE, norepinephrine.

and the Simpson index (MOO-L, P>0.05; MOO-M, P<0.05; MOO-H, P<0.01; fluoxetine, P<0.01) was significantly lower, suggesting a relative increase in microbial richness. These results suggested that MOOs could increase the richness and diversity of gut microbiota in mice.

The β-diversity analysis compared species composition across microbial communities from different samples. For β-diversity analysis, principal coordinates analysis (PCoA) and non-metric multidimensional scaling (NMDS) were used to explore similarities or differences in community composition among the six sets of samples, and the coordinate plots were drawn. The closer the sample points were to each other, the more similar the samples were. One of the key parameters in NMDS is the stress coefficient; a stress value <0.2 indicates that the NMDS analysis is reliable. The β-diversity results showed that the NMDS stress value was 0.058 (Fig. 6G), which is <0.2, indicating that the results were significant. At the OTU level, PCoA and NMDS analyses showed that the microbial communities in each group were relatively visibly clustered, and the microbial communities in the control group and the CORT group were farther away and distributed in different areas, indicating that the control group and the CORT group had notably different microbial communities (Fig. 6F). In mice treated with MOOs and fluoxetine, the distribution of the microbial communities became closer to that of the control group in a dose-dependent manner, which was similar to the results obtained in the Anosim and Adonis analyses. These results suggested that MOOs positively influenced the composition of the CORT-induced gut microbiota dysbiosis.

MOOs modulate the composition of the CORT-induced dysbiosis in mice. To investigate the effects of MOOs on species composition and species abundance in CORT-induced mouse gut microbiota, species composition and abundance were assessed using species relative abundance histograms, which were generated based on the richness data of the top 10 genera in terms of their mean abundance. Differential species were analysed for each group. Portal-level analysis showed that the mouse gut microbiota consisted primarily of four dominant phyla, namely Bacteroidota, Firmicutes, Actinobacteriota and Proteobacteria, which accounted for >98% of the total in all groups (Fig. 7A). Compared with the control group, mice in the CORT group exhibited a significantly higher relative abundance of Bacteroidota (P<0.01; Fig. 7C), and a significantly lower relative abundance of Firmicutes (P<0.01; Fig. 7D) and Actinobacteriota (P<0.01; Fig. 7E). Compared with the CORT group, mice treated with medium and high doses of MOOs and fluoxetine exhibited a significantly lower relative abundance of Bacteroidota (MOO-L, P>0.05; MOO-M, P<0.01; MOO-H, P<0.01; fluoxetine, P<0.01), and a significantly higher relative abundance of Firmicutes (MOO-L, P>0.05; MOO-M, P<0.01; MOO-H, P<0.01; Fluoxetine, P<0.01) and Actinobacteriota (MOO-L, P>0.05; MOO-M, P<0.05; MOO-H, P<0.01; Fluoxetine, P<0.01). These results suggested that MOOs had a positive regulatory effect on gut microbiota disorders in mice.

Genus-level analysis revealed that *Lactobacillus*, *Ligilactobacillus* and *Dubosiella* were the three dominant genera in the gut microbiota of mice (Fig. 7B). Compared with the control group, mice in the CORT group exhibited a decrease in the relative abundance of *Lactobacillus* (P<0.01; Fig. 7F) and *Ligilactobacillus* (P<0.01; Fig. 7G), and an increase in relative abundance of *Dubosiella* (P<0.01; Fig. 7H). Compared with the CORT group, the mice administered high doses of MOOs and fluoxetine exhibited an increase in the relative abundance of *Lactobacillus* (MOO-L, P>0.05; MOO-M, P<0.01; MOO-H, P<0.01; Fluoxetine, P>0.05) and *Ligilactobacillus* (MOO-L, P>0.05; MOO-M, P>0.05; MOO-H, P<0.01; Fluoxetine, P<0.01). The relative abundance of *Dubosiella* was decreased (MOO-L, P<0.01; MOO-M, P<0.01; MOO-H, P<0.01; Fluoxetine, P<0.01). These results suggested that MOOs partially restored gut microbiota disorders by influencing the composition of the mouse gut microbiota.

LDA and LDA effect size (LEfSe) analysis were used to further identify species that differed significantly among

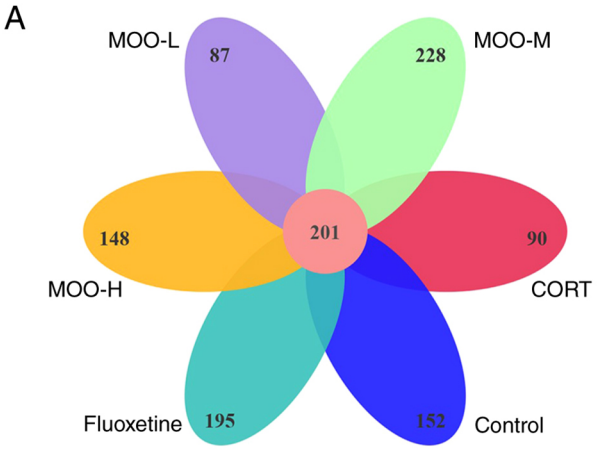

B

P value	Anosim	Adonis
Control-CORT	0.010	0.003
CORT-MOO-L	0.214	0.235
CORT-MOO-M	0.015	0.02
CORT-MOO-H	0.005	0.003
CORT-Fluoxetine	0.005	0.006
CORT-Wuzi pill	0.587	0.413

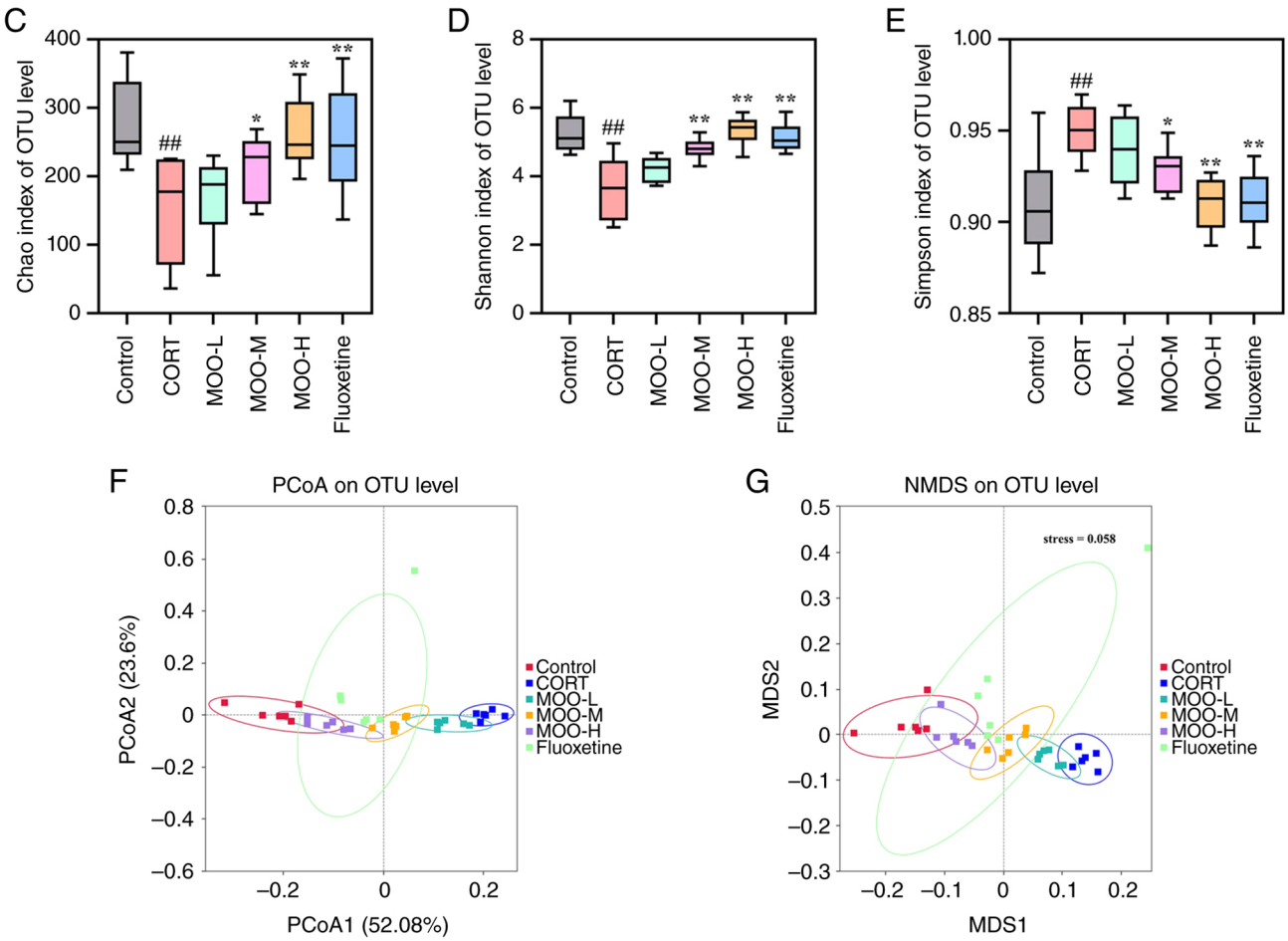

Figure 6. MOOs modulate the diversity of CORT-induced dysbiosis in mice. (A) Petal plot. (B) Anosim and Adonis analyses based on Bray-Curtis distance values. α-diversity indices reflecting microbial community richness and diversity: (C) Chao index, (D) Shannon index and (E) Simpson index. (F) Weighted unifrac distance-based PCoA. (G) Weighted unifrac distance-based NMDS. n=6. P<0.05 was considered to indicate a statistically significant difference. ##P<0.01 compared with the control group. *P<0.05 and **P<0.01 compared with the CORT group. Adonis, permutational multivariate analysis of variance; Anosim, analysis of similarities; CORT, corticosterone; MOO, *Morinda officinalis* oligosaccharide; MOO-H, high-dose MOO; MOO-L, low-dose MOO; MOO-M, medium-dose MOO; NMDS, non-metric multidimensional scaling; OTU, operable taxonomic unit; PCoA, principal coordinates analysis; unifrac.

groups and to determine the dominant organisms in each group. The results of the LEfSe analysis consisted of LDA score distribution histograms and evolutionary branching plots. With the LDA score histogram showing the effect size of differentially enriched taxa (Fig. 7I) and the cladogram visualizing their phylogenetic distribution across taxonomic levels (Fig. 7J). The results of LEfSe analysis identified 18 differentially abundant taxa (LDA>4) in the present study. *Lactobacillus* was the dominant genus in the control group, *Negativibacillus* was the dominant genus in the CORT group, *Parasutterella* was the dominant genus in the MOO-L group, *Ligilactobacillus* was the dominant genus in the MOO-H group and *Clostridium_senus_stricto_1* was the dominant genus in the fluoxetine group.

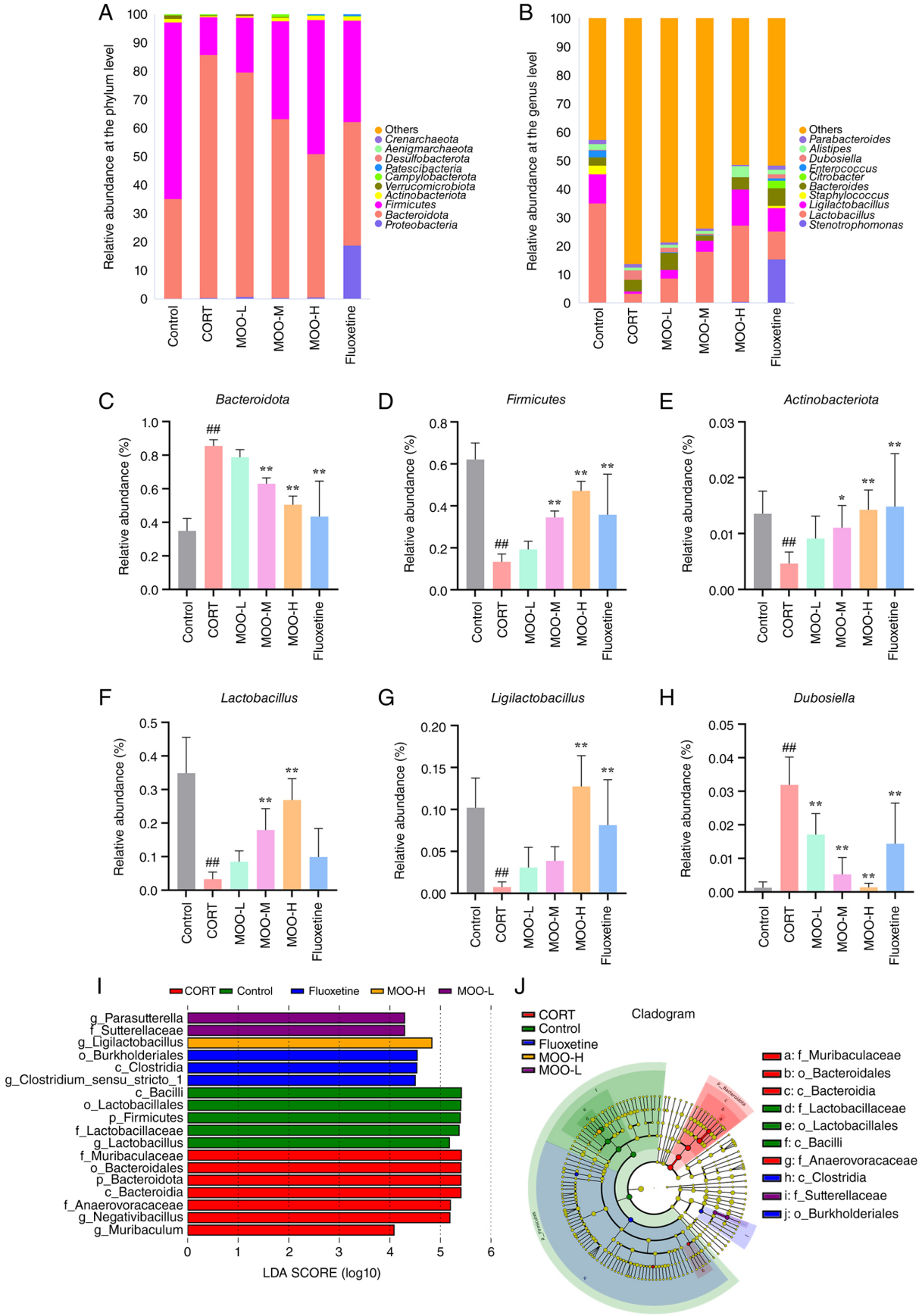

Figure 7. MOOs regulate the composition of CORT-induced gut dysbiosis in mice. (A) Analysis of differences in gut microbiota composition at the phylum level. (B) Analysis of differences in gut microbiota composition at the genus level. Relative abundance of (C) Bacteroidota, (D) Firmicutes and (E) Actinobacteriota at the phylum level. Relative abundance of (F) *Lactobacillus*, (G) *Ligilactobacillus* and (H) *Dubosiella* at the genus level. Linear discriminant analysis Effect Size analysis of (I) LDA score distribution histograms and (J) evolutionary branching maps. $^{\#\#}$P<0.01 compared with the control group. *P<0.05 and **P<0.01 compared with the CORT group. CORT, corticosterone; LDA, linear discriminant analysis; MOO, *Morinda officinalis* oligosaccharide; MOO-H, high-dose MOO; MOO-L, low-dose MOO; MOO-M, medium-dose MOO.

Discussion

Depression, a common mental illness, has a complex pathogenesis. MOOs, which are active substances in the Chinese herb *Morinda officinalis*, exhibit potential as a functional food (10,33). In the present study, SPT, FST and NSFT were used as indicators of depressive behaviours in mice to determine the effects of MOOs in terms of alleviating depressive behaviours in the CORT model. In general, a decrease in the sucrose preference rate, as well as an increase in immobilisation time and ingestion latency, are considered signs of depression (34). In the present study, 35 days of MOO treatment significantly improved CORT-induced depression-like behaviour in mice in behavioural tests.

In animal models of depression, the hippocampus is involved in the pathogenesis of depression and is the most widely studied region of the brain (35,36). Typically, pathological structural abnormalities and neurogenic dysfunction are present in the hippocampus of animal models and depressed patients (37,38). Nissl staining is frequently used to assess neuronal viability, as the number of Nissl bodies is considerably reduced in damaged neurons (39,40). Furthermore, NeuN is a key neuron-specific nuclear protein used as a marker for mature neurons, and its absence of expression implies diminished neuronal viability (41,42). There is evidence that fewer neural progenitor cells and mature granule neurons and lower numbers of granule neurons are observed postmortem in the hippocampal DG of depressed patients who have not received medication (43,44). Stress exposure-induced reductions in neurogenesis have been observed in depressed patients and rodent models of depression, and this change was reversed by long-term administration of antidepressant medication over a period of several weeks (45). In the present study, CORT markedly downregulated the expression of neuron-specific markers in the hippocampus and exacerbated neuronal damage. , whereas MOO administration restored structural and functional integrity, resulting in increased expression of hippocampal neurogenesis markers, suggesting that the neuroprotective effects of MOOs are associated with the improvement of hippocampal neurogenesis.

The development of depression may be closely associated with an abnormal deficiency of monoaminergic neurotransmitters, and defective 5-HT function is an important cause of depression (46). Damage to neurons in the DG region of the hippocampus has been reported to decrease the number of neuronal synapses, leading to diminished neurotransmission and, in turn, depressive episodes (47). Previously, reduced monoamine neurotransmission between neuronal synapses has been shown to contribute to the development of depression (48,49). Depression is typically accompanied by neuronal damage in the hippocampus; this damage leads directly to decreased levels of monoamine neurotransmitters, such as 5-HT and NE, between neuronal synapses (50). At the molecular level, MOOs serve a role in the upregulation of aminohydroxylase activity and the downregulation of 5-HT decarboxylase activity in the intestines, leading to the synthesis and enrichment of 5-HT in the brain, and thus, exerting antidepressant effects (51). In the present study, MOO treatment at medium and high doses increased the levels of the neurotransmitters 5-HT, DA and NE in the hippocampus in a significant, dose-dependent manner. Thus, MOOs have the potential to ameliorate neuronal damage in mice, thereby increasing neurotransmitter levels and exhibiting antidepressant effects.

Depression and chronic stress are associated with altered synaptic plasticity. BDNF, a key determinant of neuroplasticity highly expressed in the hippocampus, is associated with neurogenesis, neuronal differentiation and synaptic plasticity (33,52). Increasing evidence suggests that decreased levels of BDNF and its receptor TrkB in brain tissues of depressed patients, which downregulate BDNF/TrkB signalling, can lead to reduced synaptic development as well as plasticity and induce depression (53,54). Direct injection of BDNF into the hippocampus has been reported to improve depression-like behavioural changes in depressed mice (55). *Lepidium meyenii* Walp-derived extracellular vesicles enhance the release of 5-HT by modulating the gut-brain axis to increase serum 5-HT levels, and 5-HT improves BDNF expression, a key regulator of neuronal plasticity, by modulating GTP-cell division cycle 42/ERK pathway activation and activating the BDNF/TrkB/AKT signalling pathway, thereby improving depressive behaviour (56). In another study, deep brain stimulation of the nucleus ambiguus mediated the dopaminergic pathway by increasing the expression levels of BDNF, which resulted in the enhancement of the expression of DA D1 receptors and DA D2 receptors in several brain regions, including the nucleus ambiguus and ventral hippocampus, which resulted in altered functional brain connectivity to promote synaptogenesis, thereby ameliorating the mood deficits in major depressive disorder (57). Consistent with the findings of the present study, rice protein peptide treatment enhances BDNF expression by upregulating the BDNF/TrkB/CREB signalling pathway, thereby improving depressive behaviour (58). These results suggest that MOO modulation of the BDNF/TrkB/CREB signalling pathway may involve other mechanisms, such as modulation of the 5-HTergic and dopaminergic systems and provide a molecular basis for the improvement of synaptic plasticity and enhancement of neurogenesis in hippocampal neurons.

Generally, depression is associated with ecological dysregulation of the gut microbiota, which is widely recognised as a target for the treatment of depression (59,60). 16S sequencing analysis showed that MOOs restored the structure of the gut microbiota and increased the abundance and diversity of the CORT-induced gut microbiota dysregulation. In the present study, MOO intervention elevated the abundance of *Lactobacillus* and *Ligilactobacillus*, and decreased the abundance of *Dubosiella*, with the effect increasing with higher MOO doses. *Lactobacillus* and *Bifidobacterium*, representatives of probiotics, have been shown to increase the expression levels of tryptophan hydroxylase 1 in the gut, and this enhancement led to an increase in the synthesis of 5-hydroxytryptophan, and subsequently promoted the release of 5-HT (61), resulting in anxiolytic and antidepressant effects. A related study showed that oral administration of *Lactobacillus* ameliorated depressive states in mice, with *Lactobacillus* supplementation increasing hippocampal BDNF levels and exerting antidepressant effects (62). These results suggest that the gut microbiota may be an important target for intervention in depression and that MOO intervention remodelled the composition of the mouse gut microbiota,

increasing the abundance of beneficial bacteria and serving a beneficial role in modulating CORT-induced gut microbiota dysregulation in mice. Targeting the gut microbiota with therapeutic strategies holds promise for enhancing the effectiveness of pharmacologic treatments for depression. Our previous study demonstrated that MOOs alleviated chronic unpredictable mild stress (CUMS)-induced depression and sexual dysfunction via the BDNF pathway and gut microbiota remodeling (63). The present study achieved breakthroughs in model selection and mechanistic depth: The CORT-induced depression model, which complements the CUMS model, was employed, and the universality of the antidepressant effects of MOOs was validated. By combining hippocampal neuronal morphological identification and gut microbiota structural remodelling analysis, the present study systematically revealed a novel mechanism by which MOOs exerted antidepressant effects by synergistically repairing neuronal integrity and regulating the gut microbiota, providing more targeted scientific evidence for the clinical translation of MOOs.

In summary, the results of the present study suggest that MOOs attenuated CORT-induced depression-like behaviours exhibited by mice as assessed by SPT, FST and NSFT. This effect was achieved through a synergistic interaction between the BDNF/TrkB/CREB signalling pathway and 5-HT regulation. MOOs ameliorated neuronal damage in the hippocampus of mice by modulating the BDNF/TrkB/CREB signalling pathway, which in turn increased the levels of neurotransmitters in the hippocampus. In addition, MOOs regulated the composition and distribution of gut microbiota, thereby exerting further antidepressant effects. Overall, these findings suggested that MOO treatment may be a promising strategy for intervention and prevention of depression. Although the therapeutic efficacy of this approach was demonstrated in animal models of depression, further studies are required to investigate the underlying molecular mechanisms.

Acknowledgements

Not applicable.

Funding

The present study was supported by the Academic Research Projects of Beijing Union University (grant no. ZK10202204), the Open Research Fund of Beijing Key Laboratory of Bioactive Substances and Functional Foods, Beijing Union University (grant no. SWHX202105), the State Administration for Market Regulation Science and Technology Plan Project (grant no. 2023MK215), and the National Science and Technology Major Project (grant no. 2014ZX09301307).

Availability of data and materials

The raw sequencing data generated in the present study may be found in the Genome Sequence Archive of the National Genomics Data Center, China National Center for Bioinformation/Beijing Institute of Genomics, Chinese Academy of Sciences, under accession number CRA041416 or at the following URL: https://ngdc.cncb.ac.cn/gsa/search?searchTerm=CRA041416. The other data generated in the present study may be requested from the corresponding author.

Authors' contributions

YS, XD and QL conceived the study and supervised the project. MH, ZL and YC performed the experiments. ZZ, XW and SW analyzed the data. MH wrote the manuscript. XW and YS confirm the authenticity of all the raw data. All authors contributed to editorial changes of important content. All authors have participated sufficiently in the work and agreed to be accountable for all aspects of the work. All authors have read and approved the final version of the manuscript.

Ethics approval and consent to participate

The present study was approved by the Health Food Functional Testing Centre of the College of Applied Arts and Sciences of Beijing Union University (approval no. JCZX11-2404-1), Beijing, China.

Patient consent for publication

Not applicable.

Competing interests

ZZ and XW are employees of Beijing Tongrentang Company Limited, which supplied the MOO capsules used in the present study. The other authors declare that they have no competing interests.

References

1. Zhang S, Hu Y, Zhao Y, Feng Y, Wang X, Miao M and Miao J: Molecular mechanism of Chang Shen Hua volatile oil modulating brain cAMP-PKA-CREB pathway to improve depression-like behavior in rats. Phytomedicine 130: 155729, 2024.
2. Zhang HL, Sun Y, Wu ZJ, Yin Y, Liu RY, Zhang JC, Zhang ZJ, Yau SY, Wu HX, Yuan TF, *et al*: Hippocampal PACAP signaling activation triggers a rapid antidepressant response. Mil Med Res 11: 49, 2024.
3. Chen H, Shi X, Liu N, Jiang Z, Ma C, Luo G, Liu S, Wei X, Liu Y and Ming D: Photobiomodulation therapy mitigates depressive-like behaviors by remodeling synaptic links and mitochondrial function. J Photochem Photobiol B 258: 112998, 2024.
4. Zou T, Sugimoto K, Zhao Y, Li B, Zhou X and Peng C: Zhi-zi-chi decoction mitigates depression by enhancing lncRNA Six3os1 expression and promoting histone H3K4 methylation at the BDNF promoter. J Cell Mol Med 28: e18365, 2024.
5. Li S, Qian Q, Xie Y, Wu Z, Yang H, Yin Y, Cui Y and Li X: Ameliorated effects of fucoidan on dextran sulfate Sodium-Induced ulcerative colitis and accompanying anxiety and depressive behaviors in aged C57BL/6 mice. J Agric Food Chem 72: 14199-14215, 2024.
6. Xie S, Wang C, Song J, Zhang Y, Wang H, Chen X and Suo H: *Lacticaseibacillus rhamnosus* KY16 improves depression by promoting intestinal secretion of 5-HTP and altering the gut microbiota. J Agric Food Chem 72: 21560-21573, 2024.
7. He L, Mo X, He L, Ma Q, Cai L, Zheng Y, Huang L, Lin X, Wu M, Ding W, *et al*: The role of BDNF transcription in the antidepressant-like effects of 18β-glycyrrhetinic acid in a chronic social defeat stress model. Phytomedicine 132: 155332, 2024.
8. Guo X, Su L, Shi M, Sun L, Chen W, Geng J, Li J, Zong Y, He Z and Du R: Network pharmacology and transcriptomics to explore the pharmacological mechanisms of 20(S)-Protopanaxatriol in the treatment of depression. Int J Mol Sci 25: 7574, 2024.

9. Zeng H, Jiang Y, Yin Q, Li X, Xiong Y, Li B, Xu X, Hu H and Qian G: Sinisan alleviates Stress-Induced intestinal dysfunction and depressive-like behaviors in mice with irritable bowel syndrome by enhancing the intestinal barrier and modulating Central 5-hydroxytryptamine. Int J Mol Sc 25: 10262, 2024.
10. Yang L, Ao Y, Li Y, Dai B, Li J, Duan W, Gao W, Zhao Z, Han Z and Guo R: *Morinda officinalis* oligosaccharides mitigate depression-like behaviors in hypertension rats by regulating Mfn2-mediated mitophagy. J Neuroinflammation 20: 31, 2023.
11. Li Z, Xu H, Xu Y, Lu G, Peng Q, Chen J, Bi R, Li J, Chen S, Li H, *et al*: *Morinda officinalis* oligosaccharides alleviate depressive-like behaviors in post-stroke rats via suppressing NLRP3 inflammasome to inhibit hippocampal inflammation. CNS Neurosci Ther 27: 1570-1586, 2021.
12. Xu LZ, Xu DF, Han Y, Liu LJ, Sun CY, Deng JH, Zhang RX, Yuan M, Zhang SZ, Li ZM, *et al*: BDNF-GSK-3β-β-catenin pathway in the mPFC is involved in antidepressant-like effects of *Morinda officinalis* oligosaccharides in rats. Int J Neuropsychopharmacol 20: 83-93, 2017.
13. Pan SM, Yin XY, Dai DM, Zhang LW, Qi Q, Wang PJ, Hui L and Zhu ZH: Unraveling the potential of *Morinda officinalis* oligosaccharides as an adjuvant of escitalopram in depression treatment and exploring the underlying mechanisms. J Ethnopharmacol 328: 118124, 2024.
14. Chi L, Khan I, Lin Z, Zhang J, Lee MYS, Leong W, Hsiao WLW and Zheng Y: Fructo-oligosaccharides from *Morinda officinalis* remodeled gut microbiota and alleviated depression features in a stress rat model. Phytomedicine 67: 153157, 2020.
15. Zhu ZH, Yin XY, Xu TS, Tao WW, Yao GD, Wang PJ, Qi Q, Jia QF, Wang J, Zhu Y and Hui L: *Morinda officinalis* oligosaccharides mitigate chronic mild stress-induced inflammation and depression-like behaviour by deactivating the MyD88/PI3K pathway via E2F2. Front Pharmacol 13: 855964, 2022.
16. Zhu Z, Cheng Y, Han X, Wang T, Zhang H, Yao Q, Chen F, Gu L, Yang D, Chen L and Zhao Y: 20(S)-Protopanaxadiol exerts antidepressive effects in chronic Corticosterone-induced rodent animal models as an activator of Brain-type creatine kinase. J Agric Food Chem 72: 10376-10390, 2024.
17. Wang G, Cao L, Li S, Zhang M, Li Y, Duan J, Li Y, Hu Z, Wu J, Ni J, *et al*: Gut microbiota dysbiosis-mediated ceramides elevation contributes to corticosterone-induced depression by impairing mitochondrial function. NPJ Biofilms Microbiomes 10: 111, 2024.
18. Xie X, Shen Q, Ma L, Chen Y, Zhao B and Fu Z: Chronic corticosterone-induced depression mediates premature aging in rats. Affect Disord 229: 254-261, 2018.
19. Díaz L, Zambrano E, Flores ME, Contreras M, Crispín JC, Alemán G, Bravo C, Armenta A, Valdés VJ, Tovar A, *et al*: Ethical considerations in animal research: The principle of 3R's. Rev Invest Clin 73: 199-209, 2020.
20. Garcia-Garcia AL, Navarro-Sobrino M, Pilosof G, Banerjee P, Dranovsky A and Leonardo ED: 5-HT 1A agonist properties contribute to a robust response to vilazodone in the novelty suppressed feeding paradigm. Int J Neuropsychopharmacol 19: pyw057, 2016.
21. Shao Q, Li Y, Jin L, Zhou S, Fu X, Liu T, Luo G, Du S and Chen C: Semen Cuscutae flavonoids activated the cAMP-PKA-CREB-BDNF pathway and exerted an antidepressant effect in mice. Front Pharmacol 15: 1491900, 2024.
22. Chen SC, Chen YH, Song Y, Zong SH, Wu MX, Wang W, Wang H, Zhang F, Zhou YM, Yu HY, *et al*: Upregulation of phosphodiesterase 7A contributes to concurrent pain and depression via inhibition of cAMP-PKA-CREB-BDNF signaling and neuroinflammation in the hippocampus of mice. Int J Neuropsychopharmacol 27: pyae040, 2024.
23. Gao YN, Pan KJ, Zhang YM, Qi YB, Chen WG, Zhou T, Zong HC, Guo HR, Zhao JW, Liu XC, *et al*: Tofacitinib prevents depressive-like behaviors through decreased hippocampal microgliosis and increased BDNF levels in both LPS-induced and CSDS-induced mice. Acta Pharmacol Sin 46: 353-365, 2025.
24. Yao C, Jiang N, Sun X, Zhang Y, Pan R, He Q, Chang Q and Liu X: Effects of inulin-type oligosaccharides (JSO) from *Cichorium intybus* L. on behavioral deficits induced by chronic restraint stress in mice and associated molecular alterations. Front Pharmacol 15: 1484337, 2024.
25. Yang C, Chen J, Tang J, Li L, Zhang Y, Li Y, Ruan C and Wang C: Study on the Mechanism of *Dictyophora duplicata* Polysaccharide in reducing depression-like behavior in mice. Nutrients 16: 3785, 2024.
26. Liu J, Han C, Shen J, Lin Y, Shen H and Wang G: Acrylamide exposure promotes the progression of depression-like behavior in mice with CUMS via GSDMD-mediated pyroptosis. Ecotoxicol Environ Saf 289: 117443, 2024.
27. He H, Zhang X, He H, Xu G, Li L, Yang C, Liu YE, You Z and Zhang J: Microglial priming by IFN-γ involves STAT1-mediated activation of the NLRP3 inflammasome. CNS Neurosci Ther 30: e70061, 2024.
28. Wu CY, Zhang Y, Howard P, Huang F and Lee RH: ACSL3 is a promising therapeutic target for alleviating anxiety and depression in Alzheimer's disease. Geroscience 47: 2383-2397, 2025.
29. Luo F, Liu L, Guo M, Liang J, Chen L, Shi X, Liu H, Cheng Y and Du Y: Deciphering and targeting the ESR2-miR-10a-5p-BDNF axis in the prefrontal cortex: Advancing postpartum depression understanding and therapeutics. Research (Wash D C) 7: 0537, 2024.
30. Tang Y, Su H, Nie K, Wang H, Gao Y, Chen S, Lu F and Dong H: Berberine exerts antidepressant effects in vivo and in vitro through the PI3K/AKT/CREB/BDNF signaling pathway. Biomed Pharmacother 170: 116012, 2024.
31. Stein G, Aly JS, Lange L, Manzolillo A, Riege K, Brancato A, Hübner CA, Turecki G, Hoffmann S and Engmann O: Npbwr1 signaling mediates fast antidepressant action. Mol Psychiatry 30: 1828-1835, 2025.
32. Sun Y, Zhao H, Chang M, Yue T, Yuan Y and Shi Y: Prophylactic effects of Tibetan goat kefir on depression-like behaviors in chronic unpredictable stress model through the gut-brain axis. J Sci Food Agric 105: 266-275, 2025.
33. Zhang ZW, Gao CS, Zhang H, Yang J, Wang YP, Pan LB, Yu H, He CY, Luo HB, Zhao ZX, *et al*: *Morinda officinalis* oligosaccharides increase serotonin in the brain and ameliorate depression via promoting 5-hydroxytryptophan production in the gut microbiota. Acta Pharm Sin B 12: 3298-3312, 2022.
34. Arias HR, Rudin D, Luethi D, Valenta J, Leśniak A, Czartoryska Z, Olejarz-Maciej A, Doroz-Płonka A, Manetti D, De Deurwaerdère P, *et al*: The psychoplastogens ibogaminalog and ibogainalog induce antidepressant-like activity in naïve and depressed mice by mechanisms involving 5-HT2A receptor activation and serotonergic transmission. Prog Neuropsychopharmacol Biol Psychiatry 136: 111217, 2024.
35. Shen SY, Liang LF, Shi TL, Shen ZQ, Yin SY, Zhang JR, Li W, Mi WL, Wang YQ, Zhang YQ and Yu J: Microglia-derived Interleukin-6 triggers astrocyte apoptosis in the hippocampus and mediates depression-like behavior. Adv Sci (Weinh) 12: e2412556, 2025.
36. Li X, Teng T, Yan W, Fan L, Liu X, Clarke G, Zhu D, Jiang Y, Xiang Y, Yu Y, *et al*: AKT and MAPK signaling pathways in hippocampus reveals the pathogenesis of depression in four stress-induced models. Transl Psychiatry 13: 200, 2023.
37. Wang G, An T, Lei C, Zhu X, Yang L, Zhang L and Zhang R: Antidepressant-like effect of ginsenoside Rb1 on potentiating synaptic plasticity via the miR-134-mediated BDNF signaling pathway in a mouse model of chronic stress-induced depression. J Ginseng Res 46: 376-386, 2022.
38. Zhang XY, Zhang LM, Mi WD and Li YF: Translocator protein ligand, YL-IPA08, attenuates lipopolysaccharide-induced depression-like behavior by promoting neural regeneration. Neural Regen Res 13: 1937-1944, 2018.
39. Chen Z, Gu J, Lin S, Xu Z, Xu H, Zhao J, Feng P, Tao Y, Chen S and Wang P: Saffron essential oil ameliorates CUMS-induced depression-like behavior in mice via the MAPK-CREB1-BDNF signaling pathway. J Ethnopharmacol 300: 115719, 2023.
40. Gao Z, Lv H, Wang Y, Xie Y, Guan M and Xu Y: TET2 deficiency promotes anxiety and depression-like behaviors by activating NLRP3/IL-1β pathway in microglia of allergic rhinitis mice. Mol Med 29: 160, 2023.
41. Peng S, Su P, Liu L, Li Z, Liu Y, Tian L, Bai M, Xu E and Li Y: Formononetin ameliorates depression-like behaviors through rebalancing microglia M1/M2 polarization and inhibiting NLRP3 inflammasome: Involvement of activating PPARα-mediated autophagy. Mol Med 31: 153, 2025.
42. Dang R, Wang M, Li X, Wang H, Liu L, Wu Q, Zhao J, Ji P, Zhong L, Licinio J and Xie P: Edaravone ameliorates depressive and anxiety-like behaviors via Sirt1/Nrf2/HO-1/Gpx4 pathway. J Neuroinflammation 19: 41, 2022.
43. Yang K, Wu J, Li S, Wang S, Zhang J, Wang YP, Yan YS, Hu HY, Xiong MF, Bai CB, *et al*: NTRK1 knockdown induces mouse cognitive impairment and hippocampal neuronal damage through mitophagy suppression via inactivating the AMPK/ULK1/FUNDC1 pathway. Cell Death Discov 9: 404, 2023.

44. Gao Z, Peng J, Zhang Y, Chen Z, Song R, Song Z, Feng Q, Sun M, Zhu H, Lu X, *et al*: Hippocampal SENP3 mediates chronic stress-induced depression-like behaviors by impairing the CREB-BDNF signaling. Neuropharmacology 62: 110203, 2025.
45. Hao Y, Creson T, Zhang L, Li P, Du F, Yuan P, Gould TD, Manji HK and Chen G: Mood stabilizer valproate promotes ERK pathway-dependent cortical neuronal growth and neurogenesis. J Neurosci 24: 6590-6599, 2004.
46. Odaira-satoh T, Nakagawasai O, Takahashi K, Shimada M, Nemoto W and Tan-No K: Captopril prevents depressive-like behavior in an animal model of depression by enhancing hippocampal neurogenesis via activation of the ACE2/Ang (1-7)/Mas receptor/AMPK/BDNF pathway. Prog Neuropsychopharmacol Biol Psychiatry 136: 111198, 2024.
47. Qi X, Ying M, Wang A, Shi K, Zhong G, Lu Y, Liu C and Guo Y: Downregulation of USP9X in the DG region of the hippocampus leads to AD-Like cognitive dysfunction in mice. CNS Neurosci Ther 31: e70493, 2025.
48. Luo LY, Xue R, Wang TG, Zhang JW, Li S, Li JC, Fan QY, Dong HJ, Zhang Y and Zhang YZ: The ethanolic extract of *Osmanthus fragrans* var. thunbergii flowers ameliorates depressive-like behaviors of mice by modulating the serotonin system and suppressing neuroinflammation. Food Sci Nutr 12: 6242-6258, 2024.
49. Hao W, Ma Q, Wang L, Yuan N, Gan H, He L, Li X, Huang JC and Chen J: Gut dysbiosis induces the development of depression-like behavior through abnormal synapse pruning in microglia-mediated by complement C3. Microbiome 12: 34, 2024.
50. Meng P, Li C, Duan S, Ji S, Xu Y, Mao Y, Wang H and Tian J: Epigenetic mechanism of 5-HT/NE/DA triple reuptake inhibitor on adult depression susceptibility in early stress mice. Front Pharmacol 13: 848251, 2022.
51. Zhao M, Ren Z, Zhao A, Tang Y, Kuang J, Li M, Chen T, Wang S, Wang J, Zhang H, *et al*: Gut bacteria-driven homovanillic acid alleviates depression by modulating synaptic integrity. Cell Metab 36: 1000-1012.e6, 2024.
52. Huang LY, Liu YN, Chen J, Zhu HX, Li LL, Liang ZY, Song JX, Li YJ, Hu ZL, Demon D, *et al*: Caspase-12 is expressed in purkinje neurons and prevents Psychiatric-like behavior in mice. Mol Neurobiol 62: 1705-1719, 2025.
53. Chen B, Jin K, Dong J, Cheng S, Kong L, Hu S, Chen Z and Lu J: Hypocretin-1/Hypocretin receptor 1 regulates neuroplasticity and cognitive function through hippocampal lactate homeostasis in depressed model. Adv Sci (Weinh) 11: e2405354, 2024.
54. Md Samsuzzaman, Hong SM, Lee JH, Park H, Chang KA, Kim HB, Park MG, Eo H, Oh MS and Kim SY: Depression like-behavior and memory loss induced by methylglyoxal is associated with tryptophan depletion and oxidative stress: A new in vivo model of neurodegeneration. Biol Res 57: 87, 2024.
55. Zhao F, Piao J, Song J, Geng Z, Chen H, Cheng Z, Cui R and Li B: Traditional Chinese herbal formula, Fuzi-Lizhong pill, produces antidepressant-like effects in chronic restraint stress mice through systemic pharmacology. J Ethnopharmacol 338: 119011, 2025.
56. Kim H, Choi HS, Han K, Sim W, Suh HJ and Ahn Y: Ashwagandha (*Withania somnifera* (L.) Dunal) root extract containing withanolide A alleviates depression-like behavior in mice by enhancing the brain-derived neurotrophic factor pathway under unexpected chronic mild stress. J Ethnopharmacol 340: 119224, 2025.
57. Hong R, Luo L, Wang L, Hu ZL, Yin QR, Li M, Gu B, Wang B, Zhuang T, Zhang XY, *et al*: Lepidium meyenii Walp (Maca)-derived extracellular vesicles ameliorate depression by promoting 5-HT synthesis via the modulation of gut-brain axis. Imeta 2: e116, 2023.
58. Li SJ, Lo YC, Tseng HY, Lin SH, Kuo CH, Chen TC, Chang CW, Liang YW, Lin YC, Wang C, *et al*: Nucleus accumbens deep brain stimulation improves depressive-like behaviors through BDNF-mediated alterations in brain functional connectivity of dopaminergic pathway. Neurobiol Stress 26: 100566, 2023.
59. He Y, Tian Y, Xiong H, Deng Z, Zhang H, Guo F and Sun Y: Rice protein peptides ameliorate DSS-Induced cognitive impairment and depressive behavior in mice by modulating phenylalanine metabolism and the BDNF/TRKB/CREB pathway. J Agric Food Chem 72: 19812-19825, 2024.
60. Jia W, Ma Q, Xing R, Yang X, Liu D, Zeng H, Liu Z, Liu S, Xu W, Liu Z and Wu W: Jianghua Kucha black tea containing theacrine attenuates depression-like behavior in CUMS mice by regulating gut microbiota-brain neurochemicals and cytokines. Food Res Int 198: 115306, 2024.
61. Chang W, Guo J, Yang Y, Zou L, Fu Y, Li M, Li L, Li C, Wang X, Zhao X and Wu C: Semen Trigonellae alleviates LPS-induced depressive behavior via enhancing the abundance of *Ligilactobacillus* spp. Food Sci Nutr 12: 9414-9427, 2024.
62. Ren Q, He C, Sun Y, Gao X, Zhou Y, Qin T, Zhang Z, Wang X, Wang J, Wei S and Wang F: Asiaticoside improves depressive-like behavior in mice with chronic unpredictable mild stress through modulation of the gut microbiota. Front Pharmacol 15: 1461873, 2024.
63. He M, Hu M, Wang T, Zuo Z, Li H, Zhao Z, Hao Y, Dai X, Wang J and Sun Y: *Morinda officinalis* oligosaccharides alleviate chronic unpredictable mild stress-induced depression through the BDNF/TrkB/CREB pathway and symptoms of sexual dysfunction in mice. Front Neurosci 18: 1509543, 2025.